Proceedings of the Institute of Acoustics

MODEL TUNING OF A VIBRATING PLATE IN CONTACT WITH WATER

G Rognoni	Dept. of Engineering and Architecture, University of Trieste, Trieste, Italy
L Moro	Dept. of Ocean and Naval Architectural Engineering, Memorial University of Newfoundland, St. John's, NL, Canada
M Biot	Dept. of Engineering and Architecture, University of Trieste, Trieste, Italy

1 INTRODUCTION

The underwater environment experiences an increasing anthropogenic influence, manifesting in amplified noise pollution. Together with noise pollution, the international community concern is also growing. Jalkanen et al.[1] showed an increasing trend in underwater acoustic energy emitted by ships in most ocean areas, although by different scaling factors, between 2014 and 2020. Reversing this trend should be the primary goal of national and international jurisdictions through the creation of regulations on noise pollution control. Smith and Rigby[2] illustrated an exhaustive list of countermeasures, examining underwater noise sources, discerning principally between hydrodynamic noise generated by the propeller and noise generated by the machinery on board. These countermeasures are technical interventions aimed at making the ship quieter. There are other possible solutions, such as reducing speed, re-routing, and constant maintenance[3].

Within this context, a Ph.D. project started at the University of Trieste to study and evaluate the possibility of using acoustic metamaterials (AMM) to mitigate structural vibrations and reduce underwater radiated noise from ships. AMM constitutes innovative solutions for acoustics and vibration control, and the scientific interest around them has increased in the last twenty years. One typology of AMM is called Acoustic Black Holes (ABH). Introduced by Mironov[4] in 1988, they are now the focus of renewed interest for their potential. During the last two years, the Ph.D. activity mainly focused on exporting this technology from a laboratory to an operational environment[5]. To do this, we developed a strategy based on a series of experiments to test our prototypes on different structures, from small-scale sub-panels to large-scale ship mock-ups[6]. The first of these tests evaluated the reduction of vibration and radiated sound of a plate when four ABHs were installed. The plate was tested in two different configurations: hung in the air (dry condition) and hung with a face in contact with water (wet condition). This paper reports the preliminary results obtained on a bare plate without dampers. In particular, the paper focuses on developing a numerical model that can replicate the response of a vibrating plate when in contact with the water. The model will then be used to predict the ABH mitigation effect.

The literature on tests on plates vibrating in water is almost entirely focused on the match between experimental, analytical, and numerical modes of vibrations[7,8]. The current numerical software are able to predict the fluid contribution to the system dynamic with good accuracy; what lacks reliable data is the

quantification of the water-added damping. Water-added damping depends on many factors: change in mode-shape due to fluid pressure, vortex shedding, viscosity, flow velocity, surface roughness, the proximity of the nearby structure, and submergence level[9]. Within the listed factors, viscosity is indicated as having a major critical role in reducing vibration levels. It is assumed that dissipation due to viscosity happens at a fluid-structure interface in a thin boundary layer. We highlight the role of viscosity as the typical approach to modelling fluid-structure interaction disregards this particular quantity, which is then incorporated by means of loss factor, a dimensionless quantity often obtained from measurements[10].

The paper is organized as follows: section 2 briefly describes the theoretical and numerical modelling of fluid-structure interaction (2.1), the experimental activity carried out (2.2), and FE model (2.3), focusing on the updating logic selected for this specific case; the results obtained, the loss factor of the system, the surface velocity and the radiated pressure of the plate, are illustrated in section 3, followed by the discussion in section 4, and conclusions 5.

2 METHODS

2.1 Fluid structure interaction modelling in FEA

Fluid-structure interaction concerns physics problems involving mechanically-excited elastic structures entirely or partially submerged by a fluid. The elastic structure is generally modelled by finite elements (solids, shells, membranes, beams, rods). In contrast, the fluid can be modelled using different methods: finite elements (adopted in this paper), boundary elements, infinite elements, matrix or analytical techniques[11]. The modelling presented here is implemented in the Hexagon Actran software used for the numerical calculations in this paper. The formulation chosen for the fluid is Eulerian, meaning that a scalar, the pressure, describes the fluid response, while the elastic structure response is described by the displacement vector. Pressure in the fluid must satisfy the wave equation (Eq. 1):

$$\nabla^2 p = \frac{1}{c}\frac{\partial^2 p}{\partial t^2} \tag{1}$$

where ∇^2 is the Laplacian operator, p the pressure, and c the fluid sound speed. The fluid is treated as a compressible, inviscid, non-flowing medium; the fluid is described by volume finite elements defined using the Galerkin approach. The procedure at the base of the FE formulation used in Actran is reported in detail by Cesari[12] or Desmet and Vandepitte[13]. The fluid medium is discretized by three terms which, in analogy to the elastic structure, are called: acoustic stiffness matrix K_a, acoustic damping matrix C_a, and acoustic mass matrix M_a (Eq. 2):

$$([K_a] + j\omega[C_a] - \omega^2[M_a])\{p\} = \{F_a\} \tag{2}$$

F_a is the external force vector applied to the fluid. Although the names of these three matrixes recall those of the same components in the elastic structure FE formulation, they represent something different. The construction of these matrixes depends on the boundary conditions applied to the system in terms of pressures, introduced in Eq. 1. At the interface between fluid and elastic structure, the coupling condition generally assumed is given by Eq 3:

$$\frac{\partial \vec{v}}{\partial t} = -\frac{1}{\rho}\frac{\partial p}{\partial n} \tag{3}$$

where v is the speed of the structure's speed at the fluid interface and n indicates the direction normal to the interface. Through this condition, we can couple the external forces that structure and fluid exert on each other. The general equation we obtain (Eq. 4) expresses the Eulerian FE model for a coupled

vibroacoustic system:

$$\left(\begin{bmatrix} K_s & K_c \\ 0 & K_a \end{bmatrix} + j\omega \begin{bmatrix} C_s & 0 \\ 0 & C_a \end{bmatrix} - \omega^2 \begin{bmatrix} M_s & 0 \\ -\rho K_c^T & M_a \end{bmatrix} \right) \begin{Bmatrix} u \\ p \end{Bmatrix} = \begin{Bmatrix} F_s \\ F_a \end{Bmatrix} \tag{4}$$

The terms K_s, C_s, and M_s are the structure's stiffness, damping, and mass matrix, u indicates the displacement and F_s is the external force vector applied to the structure. The term K_c is the cross-coupling matrix linking fluid and structure, appearing in the stiffness and mass matrixes but not in the damping matrix. In the specific case of Hexagon Actran, the terms C_s and C_a in the damping matrix are the imaginary parts of K_s and M_a, respectively. It must be pointed out that M_a does not represent what is conventionally called added mass. The concept of added mass is generally applied to incompressible fluids. Under the hypotesis that there are no fluid forces applied (F_a = 0), due to incompressibility the speed of sound tends to infinite, and Ma tends to zero. The matrix $[K_c][K_a]^{-1}[K_c]^T$, which adds to M_s, is called added-mass matrix. When the fluid is compressible, an analogue matrix can be calculated, with the difference that M_a does not vanishes: $[K_c][K_a - \omega^2 M_a]^{-1}[K_c]^T$. This mass accounts for the added-mass effect.

2.2 Experimental test

A 1400 x 1000 mm, 6.35 mm thick steel plate was suspended using an elastic rope connected to four eyebolts at the four corners. The weight of the plate was 69 kg. Two tests were performed: one in air and a second in contact with water. We used a 3.66 m (12 ft) concrete squared tank. The water was approximately 3.66 m (12 ft) deep. The tests were carried out in the deep tank of the fluids lab at Memorial University of Newfoundland. The plate was excited by a PCB Piezotronics electrodynamic shaker (Model 2060E) connected through a PCB Piezotronics load cell (Model 208C02). The amplifier was a PCB Piezotronics 2050E09 model driven by a National Instruments 9260 voltage output module controlled by a LabView script. When in contact with the water, the angle of the plate was carefully controlled to maintain the most parallel possible to the liquid surface. A styrofoam boundary was created to prevent the water from flooding the dry surface. Fig. 1 shows the plate suspended on the facility. The red circle in Fig. 1a indicates the point where the force was connected, 250 mm from the longer side and 275 mm from the shorter side of the plate.

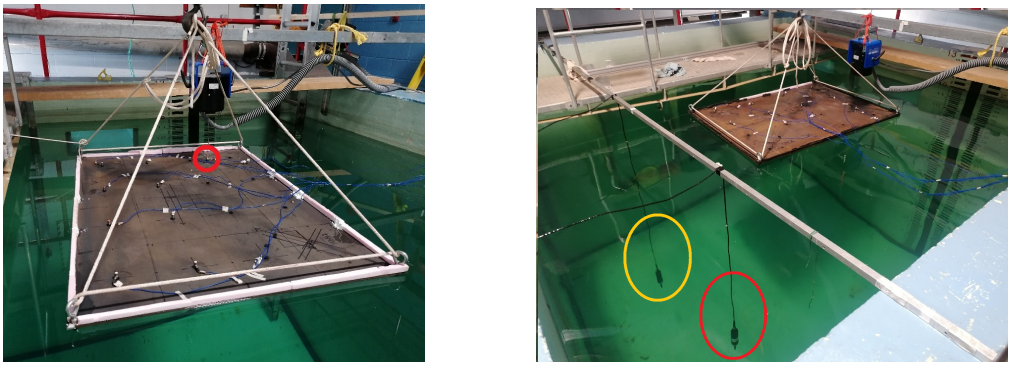

(a) ***(b)***

Figure 1: Experimental setup: a) the plate in wet condition; b) hydrophone disposition in the tank

Eight PCB Piezotronics Model 352C33 accelerometers were applied to measure the surface accelerations at sixteen different points centred on 250 x 350 mm rectangular areas. The set was divided into two subsets of eight points. It is essential to note that the sub-sets were measured in two separate sessions for operational reasons. Between one measurement and the subsequent one, the plate was lifted from its

position to allow us to change the position of the sensors. The data acquisition system used is a National Instruments 9234 analyzer. Two Ocean Sonics Model icListen RB9-ETH hydrophones were deployed in the tank to measure the underwater sound pressure. The first (P1) at a depth of 1520 mm (5 ft) and from 810 mm (32 inches) from the right end corner in both directions (red circle in Fig. 1b); the second (P2) at a depth of 2440 mm (8 ft), at 810 mm from the border parallel to the rod suspending the hydrophones and 2080 mm from the side right border (yellow circle in Fig. 1b).

2.3 FE model updating

Model updating is the process of adjusting the parameters of a finite element model to obtain reliable predictions regarding a specific desired output. The methods are a mature technology regularly used in industries such as automotive and aerospace[14]. The process of numerical updating implies the alteration of parameters that modify the response of the FE model. The chosen parameters must be selected appropriately regarding the purpose of the desired matching and proportionally to the purpose of the current investigation. Four parameterizations are typically used in the model updating process: i) the use of mass, damping, and stiffness matrix multipliers; ii) modify material properties, thicknesses, and sectional properties; iii) offsetting nodes to modify joints and boundary conditions; change FE element formulation. Generally, the criteria are based on mode frequencies and mode shapes (Modal Assurance Criterion) or the frequency response function of specific points (Frequency Response Assurance Criteria). In this case, We opted for a simpler approach, calculating, for each third-octave band between 50 and 2000 Hz, the Mean Square Velocity (MSV) value on the plate's surface and calibrating the model using this quantity. We used the exact sixteen locations as for the experiments. The 2000 Hz third-octave band was chosen as the maximum band of interest. The decision to use MSV helps facing two operational aspects: a) the frequency range of analysis we wanted to observe is wide; using an updating method considering each mode is a feasible but not proportioned way to proceed; b) obtaining the MSV for each third-octave band is practical and immediate, allowing us to streamline the procedure. This approach allowed us for a balanced effort between computational cost and accuracy of the standard.

The method used in this paper for the updating falls within the category of "Direct methods." The models obtained by this methodology reproduce the measured data exactly; they are called "representational"[15]. They replicate even noise and model inadequacies. Thus, in the representational methods, there is a requirement for accurate modelling and very high-quality measurements with some means of eliminating results from faulty sensors. Three parameters govern the plate's dynamic: elastic modulus, density, and thickness. Elastic modulus requires variations of the order of 10-20% to observe significant shifts of the peaks in the frequency MSV response; even for density, this parameter should change consistently to obtain substantial shifts in the frequency MSV response peaks. On the contrary, minor modifications significantly change the plate's frequency of MSV response when the thickness is varied. The same conclusion is also reported in literature[14]. We updated the thickness, ensuring that each third-octave band analyzed contained the same (most significant) peaks observed in the experimental response. It is not required for the experimental and numerical peaks to coincide; they must be in the same third-octave band. In this way, the energy content between the experimental and the numerical systems can be compared. Once the positions of the peaks were adjusted, we modified the loss factor attributed to the plate, which accounts for the internal damping of the steel and the water-added damping due to the fluid-structure interaction. The loss factor values were varied across the range analyzed until the matching between numerical and experimental MSV responses was satisfied for both conditions. During the updating process, we adopted a tolerance of $\pm$ 10 % between experimental and numerical values.

Two FE models were created, one for the dry condition and a second for the wet condition. The plate was modelled in Hexagon Actran by rectangular 2D elements having flexural rigidity. The average dimension of the elements' side was 19.5 mm, which, for the minimum thickness used in the analysis, leads to

a maximum discretizable frequency of approximately 2450 Hz (using eight elements per wavelength). The elastic modulus used is 206 GPa, assumed density is 7850 $\mathrm{kg/m^3}$. The plate was unconstrained, and the external force was located at the same point as in the experiment. The fluid domain elements used are tetrahedra with an average size of 40 mm, which is lower than the dimension requested for discretized waves having a frequency of 2450 Hz (70 mm using 8 elements per wavelength). The fluid density was 1000 $\mathrm{kg/m^3}$, the speed of sound was set to 1450 m/s, and the fluid damping was considered null. A frequency-dependent absorption coefficient was assigned to the tank boundaries, according to a previous study published by Fragasso et al.[16].

3 RESULTS

Fig. 2 reports two examples of acceleration response for the sixteen points in two different intervals: 2a) 190-290 Hz; 2b) 400-700 Hz. The dotted circles indicate the peaks where it was possible to evaluate the damping loss factor using the half-power bandwidth method. Fig. 3a reports the experimental average loss factor calculated for each peak between 0 and 2500 Hz for the two conditions. The half-power bandwidth method was used to calculate the loss factor for each peak in the sixteen points measured on the plate surface. These values were then averaged.

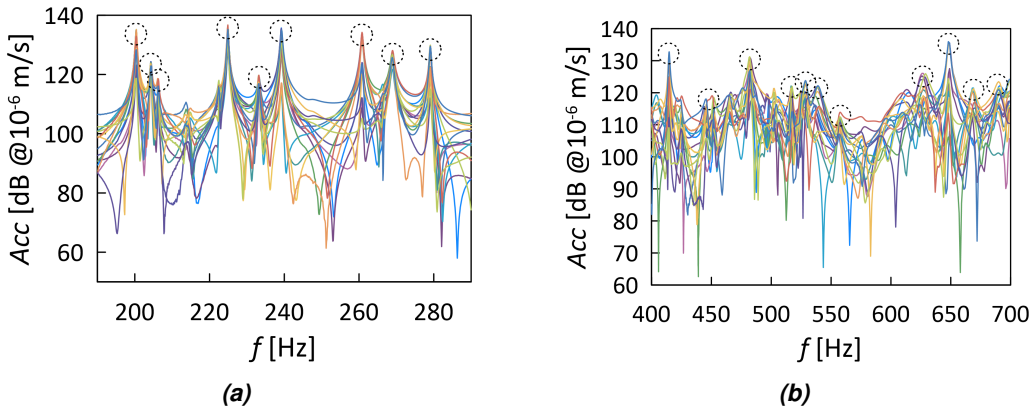

Figure 2: Accelerations measured on the plate: a) 190 - 290 Hz b) 400 - 700 Hz. The dotted circles show the peaks where it was possible to calculate the loss factor

Fig. 3b shows the loss factor values estimated for each third-octave band between 50 and 2000 Hz. The straight curves connect the experimental values (circles), and the dotted lines connect the numerical values (crosses) imputed to tune the FE model with the experimental response.

The MSV obtained experimentally and numerically is shown in Fig. 4. The dashed lines connect the numerical values obtained at the end of the tuning procedure. The values are reported for each third-octave band between 63 and 2000 Hz. The vibration, as expected, is higher in the air as the water introduces the added mass and the added damping effect. It can also be observed that the response measured in air is shifted to lower frequencies when the plate interacts with the water because of the added mass.

The updated FE model was used to predict the pressures in the same two tank points where the hydrophones were placed during the experiment. The predicted values compared with the experimental measurements for each third-octave band from 63 to 2000 Hz are shown in Fig. 5.

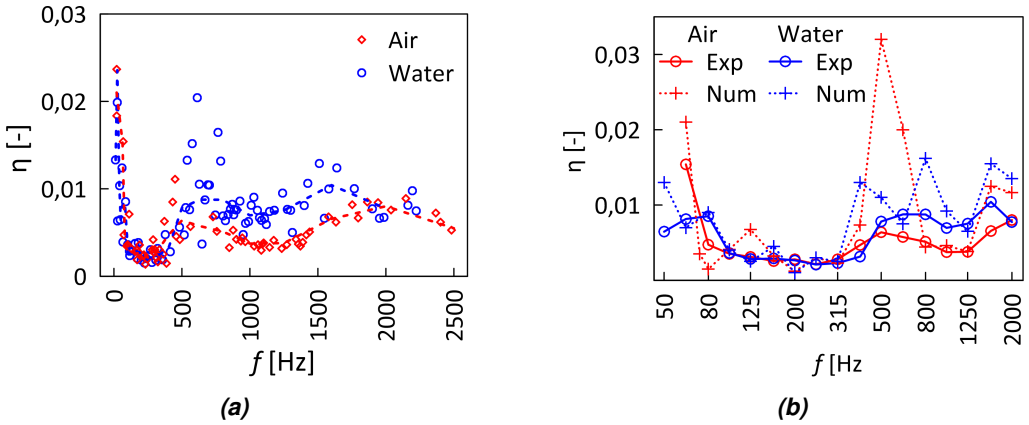

Figure 3: a) Experimental loss factor for dry and wet conditions; b) comparison between experimental and numerical loss factor

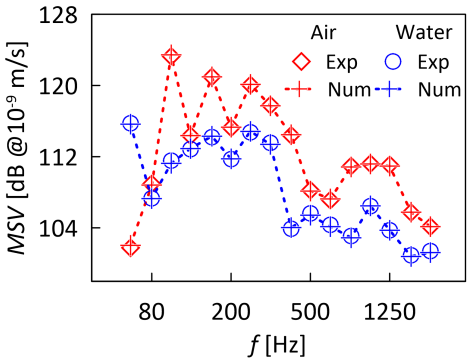

Figure 4: Comparison between the MSV in air and water: numerical and experimental response

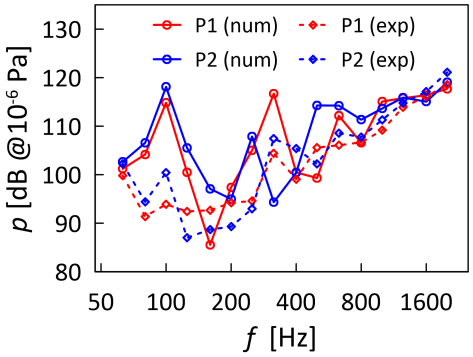

Figure 5: Sound pressure levels measured experimentally and predicted by the updated model

4 DISCUSSION

The distribution of the experimental damping loss factor values calculated for the two different conditions (Fig. 3a) highlights the presence of two ranges. In the low-medium frequency range (5 - 500 Hz), we can state that there is no difference between air and water. Differently, over 500 Hz, the loss factor for the wet condition is higher than that for the dry condition. This difference between low and high-frequency ranges indicates a different influence of the water-added damping: its effect is significant in the medium-high frequency field, while its contribution is negligible at lower frequencies. Below 500 Hz, the reduction of vibration levels observable in Fig. 4 is attributable to added mass.

With increasing frequency, experimental loss factor becomes sparser for both conditions, meaning that the measurable peaks are less (especially in the wet condition). This can be observed by comparing the graphs in Fig. 2. The circled peaks in Fig. 2a are nine in a frequency span of 100 Hz, while in Fig. 2b, we can count eleven measurable peaks in a span of 300 Hz. Founding fewer measurable peaks means that the system damping increases. For the dry condition, values are sparser between 400 and 800 Hz. For the wet condition, high damping values are expected in the range between 400 and 700 Hz and over

1000 Hz.

The numerical loss factor trend coincides with the experimental one up to the 400 Hz third-octave band (Fig. 3b); over this band, the numerical values are always equal or greater than the experimental ones. In the dry condition, we can observe a significant surge in the numerical loss factor needed to match the experimental response in the 500 Hz and 630 Hz third-octave bands. Fig. 4 shows that in this frequency range, there is a sudden drop of the plate response in the air as the damping increases. It is not clear the reason for such an increase; it can be attributed to something related to the external conditions during the experiments: resonance phenomena of the hanging system or some disturbances due to the system-shaker coupling. The numerical air loss factor curve then drops back to the experimental values in the third-octave bands between 800 and 1250 Hz and increases in the last two third-octave bands analyzed. In the wet condition, the numerical loss factor generally overcomes the experimental one over 400 Hz, except for the 630 and 1250 Hz Third-octave bands, whose values match.

The differences observed between the numerical and experimental loss factor values in the wet condition can have different explanations: i) experimentally, the half-power bandwidth method allows us to measure only the sharper peaks (at least 1-2 dB high), which can lead to underestimating the damping since I can measure it only where it is low; ii) when mode density is high, only see the most energetic modes can be seen and some of the other modes that may experiment higher levels of damping could not be measured; iii) the FE model disregards a series of effects present during the real tests: boundary conditions uncertainties, imperfections in the manufacturing, shaker-stinger-plate coupling, viscosity, unknown effects. Therefore, they must be accounted for in some other way, such as the damping.

The comparison between measured and predicted sound pressure levels in the tank (Fig. 5) shows a similar trend, which increases with increasing frequency. The experimental and numerical curves tend to get closer at high frequency, where the sound field becomes more diffuse, and the influence of acoustic anti-nodes becomes less critical. The increase of pressure radiated by the plate in the higher third-octave bands is coherent with the theory stating that the radiation efficiency increases with frequency, reaching one in correspondence with the coincidence frequency where the flexural wave number of sound waves in the plate and the wave number of those in the fluid are equal. As an indication, the radiation efficiency calculated in the same tank for a similar plate approximately reaches 1 around 1250-1500 Hz[16]. Over this frequency, we can expect the radiated sound to be proportional to the mean square velocity of the plate.

5 CONCLUSION

The paper presents the results of an experimental-numerical study on a plate vibrating in air and in contact with water. The results provide helpful information regarding installing a damping system to reduce the plate's vibration. Whether those interventions would have any effect in the medium-high frequency range, where the interaction with the water introduces significant damping effects, is questionable. We already know that solutions such as viscoelastic materials, tuned resonators, and acoustic black holes work on plates vibrating in the air. Therefore, with the damping below 500 Hz unchanged between dry and wet conditions, we expect the same systems to work even when the plate is in contact with the fluid. Over 500 Hz, however, the water-damping contribution may be so high that introducing such systems could be less effective.

In the near future, the research will focus on three main points connected to the presented paper: i) the use of different techniques to evaluate damping in the high-frequency ranges, for example, the Power Injection Method (PIM), bypassing the limitations imposed by the half-power bandwidth method; ii) present the results of the experiment performed in the tank where 1 to 4 ABHs were mounted on the plate,

discussing the results in light of the findings here presented; and, iii) develop a model to evaluate the noise radiated by the panel in open field[17];

ACKNOWLEDGMENTS

Risultati conseguiti con il finanziamento ottenuto a valere sull'Asse IV del PON Ricerca e Innovazione 2014-2020 "Istruzione e ricerca per il recupero – REACT-EU"

REFERENCES

1. J.P. Jalkanen, L. Johansson, M.H. Andersson, E. Majamäki and P. Sigray, "Underwater noise emissions from ships during 2014–2020", *Environ. Pollut.* **311**(119766). (2022).
2. T.A. Smith and J. Rigby, "Underwater radiated noise from marine vessels: A review of noise reduction methods and technology", *Ocean Eng.* **266**(112863). (2022).
3. IMO, "Revised guidelines for the reduction of underwater noise from commerical shipping to address adverse impacts on marine life". (2023).
4. M.A. Mironov, "Elastic wave propagation in a plate, thickness of which smoothly decreases to zero on a finite interval", *Akusticheskij Zhurnal* **34**(112863). 546-547. (1988).
5. G. Kyaw Oo D'Amore, G. Rognoni, M. Biot, F. Mauro, "Acoustic black holes: The new frontier for soundproofing on board ships", *Advances in the Analysis and Design of Marine Structures*. (2023).
6. G. Rognoni, G. Kyaw Oo D'Amore, E. Brocco, L. Moro, M. Biot, "Investigation on the Impact of a Metamaterial Solution for the Mitigation of Noise Radiated by a Ship Panel", *Proceedings of ISOPE Conference*. (2023).
7. A. Ergin and B. Ugurlu, "Linear vibration analysis of cantilever plates partially submerged in fluid", *J. Fluids Struct.*, **17**. 927-939. (2003)
8. W.R.Marcum, K. Britsch, P.L. Harmon, S. Liu, A. Weiss, T.K. Howard, M. Moussaoui, W.F. Jones, "Numeric benchmark study of plate vibration experiments in air and water". *Int. J. Thermofluids* **1-2**. (2020).
9. C. Trivedi, "A review on fluid structure interaction in hydraulic turbines: A focus on hydrodynamic damping", *Eng. Fail. Anal.* **77**. 1-22. (2017).
10. C. Conca, A. Osses and J. Planchard, "Added mass and damping in fluid-structure interaction", *Comput. Methods Appl. Mech. Eng.* **146**. 287-405. (1997).
11. G.C. Everstine, "Finite element formulations of structural acoustic problems", *Comput. Struct.* **65**3. 307-321. (1997).
12. F. Cesari, "Il metodo degli elementi finiti applicato al moto dei fluidi", Pitagora Editrice, Bologna (1986).
13. W. Desmet and D. Vandepitte, "Finite Element Method in Acoustics", *ISAAC13 - Internation Seminar of Applied Acoustics*, Leuven, (2002).
14. R. Allemang and P. Avitabile, *Handbook of Experimental Structural Dynamics*, Springer, New York (2022).
15. M. I. Friswell and J. E. Mottershead, *Finite Element Model Updating in Structural Dynamics*, Springer, Dordrecht (1995).
16. J. Fragasso, K.M. Helal and L. Moro, "Transfer-path analysis to estimate underwater radiated noise from onboard structure-borne sources", *Appl. Ocean Res.* **147** 103979. (2024).
17. K.M. Helal, J. Fragasso, L. Moro, "Underwater noise characterization of a typical fishing vessel from Atlantic Canada", *Ocean Eng.* **299**(117310). (2024).